A Framework for Creating Realistic Synthetic Fluorescence Microscopy Image Sequences

Matsilele Mabaso[1], Daniel Withey[1] and Bhekisipho Twala[2]

[1]MDS(MIAS), Council for Scientific and Industrial Research, Pretoria, South Africa
[2]Department of Electrical and Electronic Engineering, University of Johannesburg,
Auckland Park, Johannesburg, South Africa

Keywords: Synthetic Image Sequences, Microscopy Bioimaging, Spot Detection.

Abstract: Fluorescence microscopy imaging is an important tool in modern biological research, allowing insights into the processes of biological systems. Automated image analysis algorithms help in extracting information from these images. Validation of the automated algorithms can be done with ground truth data based on manual annotations, or using synthetic data with known ground truth. Synthetic data avoids the need to annotate manually large datasets but may lack important characteristics of the real data. In this paper, we present a framework for the generation of realistic synthetic fluorescence microscopy image sequences of cells, based on the simulation of spots with realistic motion models, noise models, and with the use of real background from microscopy images. Our framework aims to close the gap between real and synthetic image sequences. To study the effect of real backgrounds, we compared three spot detection methods using our synthetic image sequences. The results show that the real background influences spot detection, reducing the effectiveness of the spot detection algorithms, indicating the value of synthetic images with a realistic background in system validation.

1 INTRODUCTION

Advances in bioimaging based on fluorescence microscopy have become fundamental in biomedical and medical research. The use of fluorescence microscopy and specific staining methods makes the biological molecules to appear as bright particles called spots. These bright particles are local intensity maxima whose intensity level is significantly different from their neighbourhood. This technique generates a huge amount of data which is degraded by factors such as noise and non-uniformity in the background. Automated image analysis algorithms are used to study and analyse these images. Evaluation of these algorithms in real image datasets requires manual annotation to estimate the ground truth. However, the process of manual annotation requires an expert to follow hundreds of spots moving in an image sequence. This process can be tedious, susceptible to errors and the ground truth varies when repeated.

To avoid the problem of manual annotation, several studies (Genovesio et al., 2006; Sbalzarini and Koumoutsakos, 2005; Smal et al., 2010; Yoon et al., 2008; Ruusuvuori et al., 2008; Ruusuvuori et al.,

2010; Rezatifighi et al., 2013) introduced the use of synthetic image sequences to simulate real microscopy images. The use of synthetic images became popular because they contain the ground truth data and give the opportunity to compare and validate the results of automated methods. Most existing frameworks for the creation of synthetic image sequences (Feng et al., 2011; Smal et al., 2010; Smal et al., 2008) make certain assumptions, such as: no background structures, fixed shape for spots and fixed signal to noise ratio.
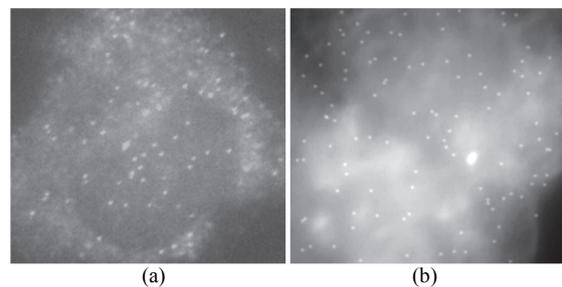

Figure 1: A selection of images with multiple spots. (a) real fluorescence microscopy image, and (b) synthetic image with a real background. The background in (b) was obtained from a different study.

These assumptions make creations of synthetic images simpler; however, they do not fully reflect the complexity of real images.

In this work, we describe a powerful framework for creating realistic synthetic image sequences. The approach presented in this study is based on the use of real microscopy image sequences, unlike other frameworks that simulate the entire image sequence. Instead of learning the background and trying to simulate it, our framework makes use of real microscopy images with synthetic spots. To simulate our spots we place a Gaussian profile directly into the real image. These will result in partially-synthetic image sequences. The proposed framework is described for 2D images but can also be extended to 3D.

This paper is organized as follows: Section 2 gives some related work, followed by Section 3 which explains the framework strategy, then Section 4 and 5 present the experimental set-up and results, and, finally, Section 6 concludes the study.

2 RELATED WORK

There exist several studies for the creation of synthetic sequences of microscopy images.

Smal (Smal, 2015) proposed a framework that can mimic images acquired using fluorescence microscopy. The procedure can simulate background structures and spots, however, it does not fully mimic the background of real images, and spot motion is not considered. Another study (Genovesio et al., 2006) generated synthetic images using a mixture of Gaussians to form the background. Their study modelled some image properties however, it lacked the properties of a real background structures. Similar to (Genovesio et al., 2006), (Yoon et al., 2008) proposed a framework which can model the movements of spots in microscopy images. However, (Yoon et al., 2008) did not take into account the background in microscopy images.

There exist few methods which can model the effects of image noise, spot motion, and realistic background in synthetic microscopy images. The work by (Smal, 2015) can model noise and background but the motion of spots was not considered. Another work by (Rezatifighi et al., 2013) uses HDome transformation (Vincent, 1993) to estimate the background in real microscopy image sequences. Although, their study can model spot motion and noise, it still lacks important characteristics of real data.

A recent study by (Chenouard et al., 2014) compared the performance of different tracking methods using synthetic image sequences. Their sequences contained spots moving in random walk with varying velocities, and Gaussian noise was used to simulate the kind of noise found in microscopy images. However, the disadvantage of their sequences is lack of background structures. One of the major conclusions in their study is the need for synthetic image sequences with realistic background.

3 OUR FRAMEWORK

To generate our realistic synthetic image sequences, we propose an improved framework as shown in, Figure 2, which is able to create realistic synthetic image sequences of fluorescence microscopy.
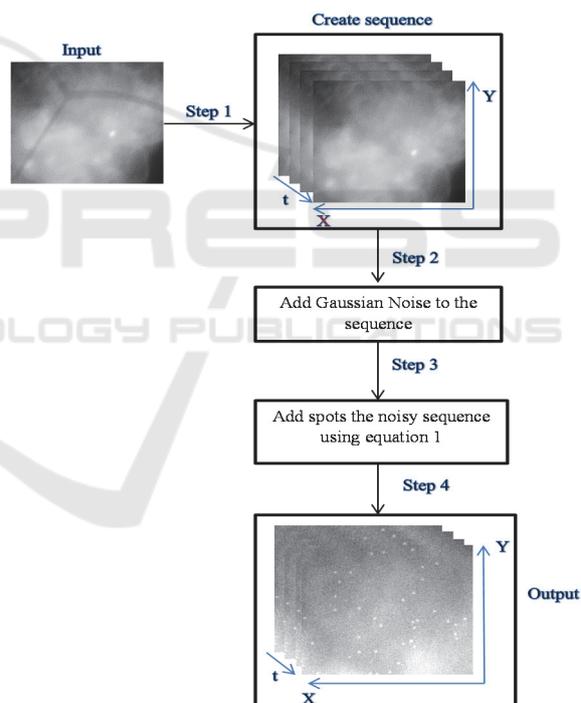

Figure 2: A diagram showing the steps involved in our framework for the creation of synthetic image sequences.

3.1 Reference Data

An example of a real microscopy image with mRNA spots is shown in Figure 1(a).

3.2 Background Modelling

Existing work on creating synthetic image sequences are based on estimating the background either by using HDome (Vincent, 1993) or Gaussian mixture model (Genovesio et al., 2006). The disadvantage of estimating the background is that it will still be different from the real background. In our framework, instead of simulating the background, we make use of real microscopy images (without spots) and add the spots. The real images were obtained from our collaborator, the Synthetic Biology Research Group at the CSIR.

3.3 Spot Model

Fluorescence microscopy images contain a number of bright particles (spots) superimposed on an uneven background, as shown in Figure(a). The most common approach to model these spots is to fit a Gaussian intensity profile (Cheezum et al., 2001; Zhang et al., 2007; Carter et al., 2005). In this work, we considered a 2D Gaussian function with four parameters, the position, x and y, standard deviation, and peak intensity. The model for a single spot is given by:

$$G(x,y) = Ie^{-\left(\frac{(x-x_0)^2}{2\sigma_x^2}+\frac{(y-y_0)^2}{2\sigma_y^2}\right)} \qquad (1)$$

The parameters, σ_x, σ_y describes the width of the spots, and, I, the spot amplitude. In order to model an isotropic spot, the parameters, σ_x and σ_y were set to be equal.

3.4 Spot Motion Models

The movements of spots in microscopy imaging can be described using some statistical models of motion. A number of studies (Genovesio et al., 2006; Feng et al., 2011; Rezatifighi et al., 2013) suggested the use of three kinds of models to describe the kinds of spot movements in microscopy images (Genovesio et al., 2006). The models include random walk, first order linear extrapolation, and second order linear extrapolation, modelling Brownian motion, constant speed, and constant acceleration movements, respectively, which are motions representative of biological motion (Lakadamyali et al., 2003). To model the movement of spots using the above mentioned motion models, we used a plugin developed by (Chenouard, 2015)

3.5 Noise Generation

There exists many noise sources in microscopy imaging which affects the image quality. To simulate the kind of noise found in microscopy imaging, we used additive Gaussian noise with mean of zero and varying standard deviation, $N \sim N(\mu = 0, \sigma_{noise})$. Gaussian models are commonly used models in microscopy imaging.

3.6 Signal to Noise Ratio

The quality of images can be expressed in terms of signal to noise ratio (SNR). The SNR measures the amount of noise in image and is widely used in image processing. The signal to noise ratio was defined as the ratio of spot intensity, I_{max}, divided by the noise standard deviation, σ_{noise};

$$SNR = \frac{I_{max}}{\sigma_{noise}} \qquad (2)$$

4 EXPERIMENTAL SET-UP

4.1 Synthetic Sequences

The framework presented in this study is capable of simulating different kinds of microscopy image sequences. In order to study the effect of real background on synthetic image sequences, we created two types of synthetic image scenarios. The first scenario consisted of image sequences with no background structures (named NOBGND) and the second scenario consisted of synthetic sequences with real fluorescence background structures. BGND refers to background. For the second scenario four realistic synthetic image sequences (named, BGND0, BGND1, BGND2 and BGND3) were created by varying the background as shown in, Figure 3, All the scenarios were corrupted by Gaussian noise, with the mean of zero and varying standard deviation {2.86, 5, 10, 20}. The following signal to noise ratios (SNR) levels were explored {7, 4, 2, 1} where the spot intensity was 20 gray levels. Each synthetic image sequence created was of 100 time steps with image dimension of 512 by 512 pixels. The density of spots in each image of a sequence was on the order of {50-100} and the spots motion models were governed by Brownian motion. The spot numbers, dynamics, start and end were randomized in order to mimic the kinds of properties in real microscopy images. MATLAB was used to

add spots, and the OMERO.matlab-4.3.3 toolbox was used to read and save images.

4.2 Detection Methods

In order to study the effect of real background on synthetic image sequence, we compared results from three spot detection methods applied to our synthetic image sequences. These methods were chosen based on their implementation availability and they were also being used in different comparison studies (Ruusuvuori et al., 2010; Smal et al., 2010). The detection algorithms compared are, Isotropic Undecimated Wavelet Transform (IUWT) (Olivo-Marin, 2008), Feature Point Detection (FPD) (Sbalzarini and Koumoutsakos, 2005) and HDome Transformation (Smal et al., 2010; Vincent, 1993). A detailed description of each method is found in Appendix A.

4.3 Performance Measure

In order to test the performance of the three detection methods, we computed several measures: true positives (TP), false positives (FP) and false negatives (FN). True positives are detected spots that correspond to the ground-truth spots. If the detected spot does not correspond to the ground truth it is considered as a false positive. A missed ground truth spot is considered as a false negative. Two performance measures are considered in this study, Recall and Precision (Allalou et al., 2010). Recall measures the ratio of correctly detected spots overall ground-truth spots, and is defined as:
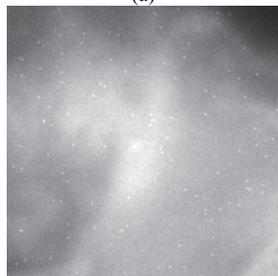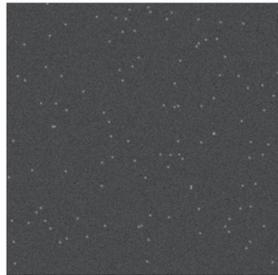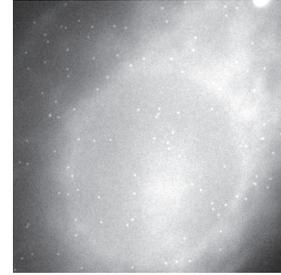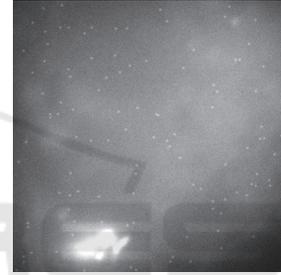

(a)

(b)
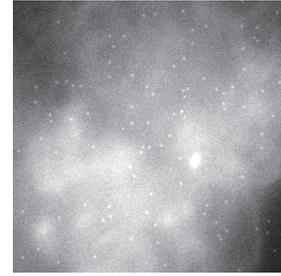
(c)

(d)

(e)

Figure 3: Examples of synthetic image sequences created using our framework. (a) NOBGND, and (b) BGND0, (c) BGND1, (d) BGND2, and (e) BGND3.

$$Recall = \frac{N_{TP}}{N_{TP} + N_{FN}} \qquad (3)$$

Precision measures the ratio of correctly detected spots among all detected spots and defined as:

$$Precision = \frac{N_{TP}}{N_{TP} + N_{FP}} \qquad (4)$$

Where N_{TP} the number of true positives is, N_{FN} is the number of false negatives and N_{FP} the number of false positives.

Then, the F_{score} measure is computed as a weighted average of the two measures, precision and recall:

$$F_{score} = 2 \times \frac{precision \times recall}{(precision + recall)} \qquad (5)$$

A good detection method should have the value of F_{score} approaching one.

5 EXPERIMENTAL RESULTS

We evaluate the performance of three detection methods using synthetic image sequences consisting of five experimental scenarios. The first scenario consisted of image sequences with no background structures, NOBGND. This will help with the evaluation of the performance of the algorithms as a function of image noise (SNR). The second to fifth scenario consisted of image sequences with a real background (BGND0, BGND1, BGND2 and BGND3). The second to fifth experimental scenarios were used to evaluate the performance of the methods as a function of real background and image noise. In all the scenarios, the spot motion was governed by Brownian motion. For each method, the performance measures, Recall, Precision and F_{score}, were computed. It's important to mention that the only difference between image scenarios was the background, and all other properties were the same.

Figure 4 shows the results of all detection methods in terms of F_{score}. The results show that all methods performed well on NOBGND sequences compared to sequences with a background. It is noted that the HDome and FPD methods fail to reach F_{score} nearly one on NOBGND test case at SNR=7; because the challenges of handling overlapping spots. It turns out that the performance of the algorithms decreases when the real background is introduced. The decrease in performance of the algorithms could be explained by the increase in the number of false positives (FP) and false negatives (FN) detected by the algorithms when the background is introduced, and thus affecting the F_{score}. In all experiments, the IUWT method performed better compared to other methods. However at SNR=2 or below all methods drop in performance for all experiments.
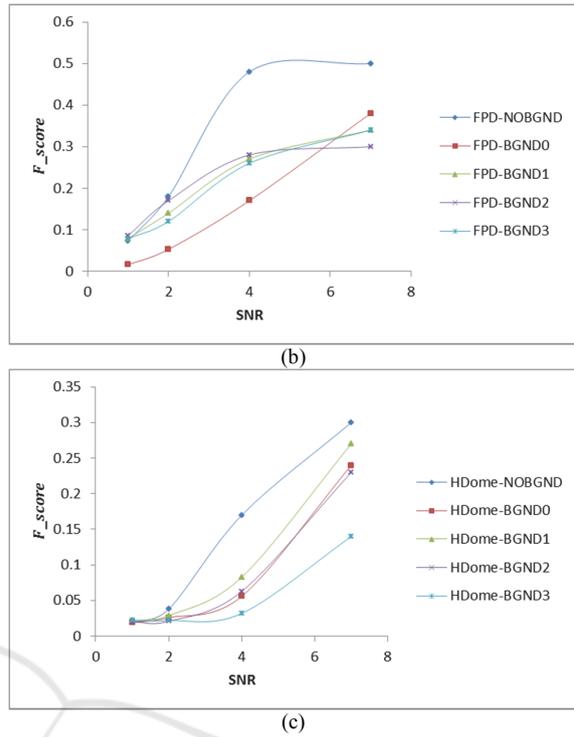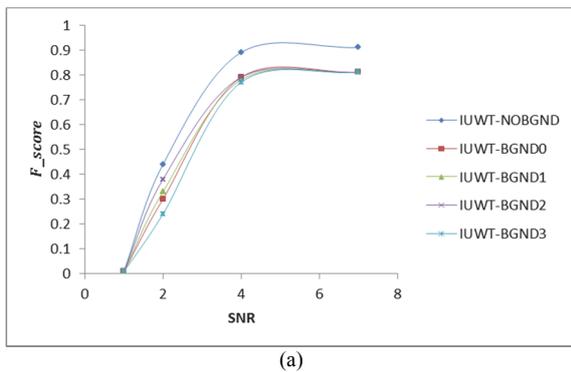

(a)

(b)

(c)

Figure 4: The curves of F_{score} versus SNR for the detection methods applied to two synthetic image scenarios as described in Section 4.1. (a) IUWT, (b) FPD and, (c) HDome. All methods perform less well with realistic background.

6 CONCLUSIONS

In this work we presented a framework for the simulation of fluorescence microscopy images sequences and also study the effect of real background on synthetic image sequences. The framework improves the modelling of real microscopy image sequences by including realistic spots, realistic noise, and realistic motion with real image background. The synthetic image sequences created using this framework offer a better way to evaluate different detection and tracking algorithms since the ground truth is available. Our evaluation results showed that the performance of three detection methods is reduced when tested with synthetic image sequences exhibiting realistic background, compared to the sequences which had no background. This showed that the real background has an effect on spot detection algorithm performance. The performance of the detection methods is reduced in the presence of background structures.

ACKNOWLEDGEMENTS

REFERENCES

Allalou, A., Pinidiyaarachchi, A. and Wählby, C. (2010) 'Robust signal detection in 3D fluorescence microscopy ', *Cytometry*, vol. 77A, no. 1, pp. 86-96.

Carter, B.C., Shubeita, G.T. and Gross, S.P. (2005) 'Tracking single particles: a user-friendly quantitative evaluation', *Physical Biology*, vol. 2, no. 1, pp. 60-72.

Cheezum, M.K., Walker, W.F. and Guilford, W.H. (2001) 'Quantitative comparison of algorithms for tracking single fluorescent particle', *Biophysical Journal*, vol. 81, pp. 2378-2388.

Chenouard, N. (2015) *Particle tracking benchmark generator*, [Online], Available: http://icy.bioimageanalysis.org/plugin/Particle_trackin g_benchmark_generator [1 September 2015].

Chenouard, N., Ihor, S., de Chaumont, F., Maska, M., Sbalzarini, I.F., Gong, Y., Cardinale, J., Carthel, C., Coraluppi, S., Winter, M., Cohen, A.R., Godinez, W.J., Rohr, K., Kalaidzidis, Y., Liang, L., Duncan, J., Shen, H., Xu, Y., Magnusson, K.E., Jalden, J. et al. (2014) 'Objective comparison of particle tracking methods', *Nature Methods*, vol. 11, no. 3, pp. 281-290.

Crocker, J.C. and Grier, D.G. (1996) 'Methods of Digital Video Microscopy for Colloidal Studies', *Journal of Colloid and Interface Science 179*, pp. 298-310.

Feng, L., Xu, Y., Yang, Y. and Zheng, X. (2011) 'Multiple dense particle tracking in fluorescence microscopy images based on multidimensional assignment', *Journal of Structural Biology*, vol. 173, pp. 219-228.

Genovesio, A., Liendl, T., Emiliana, V., Parak, W.J., Coppey-Moisan, M. and Olivo-Marin, J.-C. (2006) 'Multiple particle tracking in 3d+t microscopy: Method and application to the tracking of endocytosed quantum dots', *IEEE Transactions on Image Processing*, vol. 15, no. 5, pp. 1062-1070.

Lakadamyali, M., Rust, M.R., Babcock, H.P. and Zhuang, X. (2003) 'Visualizing infection of individual influenza viruses', Proceedings of the National Academy of Science of the United States of America, 9280-9285.

Olivo-Marin, J.-C. (2008) 'Extraction of spots in biological images using multiscale products', *Pattern Recognition*, vol. 35, no. 9, pp. 1989-1996.

Rezatifighi, S.H., Pitkeathly, W.T., Goud, S., Hartley, R., Mele, K., Hughes, W.E. and Burchfield, J.G. (2013) 'A framework for generating realistic synthetic sequences of total internal reflection fluorescence microscopy images', 10th IEEE International Symposium on Biomedical Imaging, 157-160.

Ruusuvuori, P., Äijö, T., Chowdhury, S., Garmaendia-Torres, C., Selinummi, J., Birbaumer, M., Dudley, A.M., Pelkmans, L. and Yli-Harja, O. (2010) 'Evaluation of methods for detection of fluorescence labeled subcellular objects in microscope images', *BMC Bioinformatics*, vol. 11, pp. 1-17.

Ruusuvuori, P., Lehmussola, A., Selinummi, J., Rajala, T., Huttunen, H. and Yli-Harja, O. (2008) 'Benchmark set of synthetic images for validating cell image analysis algorithms', Proceedings of the 16th European Signal Processing Conference, EUSIPCO.

Sbalzarini, I.F. and Koumoutsakos, P. (2005) 'Feature Point Tracking and Trajectory Analysis for Video Imaging in Cell Biology', *Journal of Structural Biology*, vol. 151, no. 2, pp. 182-195.

Smal, I. (2015) *Synthetic data generator*, September, [Online], Available: http://smal.ws/wp/software/synthetic-data-generator/.

Smal, I., Loog, M., Niessen, W. and Meijering, E. (2010) 'Quantitative comparison of spot detection methods in fluorescence microscopy', *IEEE Trans on Medical Imaging*, vol. 29, no. 2, pp. 282-301.

Smal, I., Meijering, E., Draegenstein, K., Galjart, N., Grigoriev, I., Akhmanova, A., van Royen, M., Houtsmuller, A.B. and Niessen, W. (2008) 'Multiple object tracking in molecular bioimaging by Rao-Blackwellized marginal particle filtering', *Medical Image Analysis* , vol. 12, no. 6, pp. 764-777.

Vincent, L. (1993) 'Morphological grayscale reconstruction in image analysis: Applications and efficient algorithms ', *IEEE Trans Image Process*, vol. 2, pp. 176-201.

Yoon, J.W., Bruckbauer, A., Fitzgerald, W.J. and Klenerman, D. (2008) 'Bayesian inference for improved single molecule fluorescence tracking', *Biophysical Journal*, vol. 94, pp. 4932-4947.

Zhang, B., Zerubia, J. and Olivo-Marin, J.-C. (2007) 'Gaussian approximations of fluorescence microscope PSF models', *Applied Optics*, vol. 46, no. 10, pp. 1-34.

APPENDIX-A

Spot Detection Methods

Isotropic Undecimated Wavelet Transform

The method of IUWT was proposed in (Olivo-Marin, 2008) for the detection of spots in biological images. The algorithm is based on the assumption that spots will be present at each scale of wavelet decomposition and thus will appear in the multiscale product. The á trous wavelet transform step is based on the convolution of the image $I(x, y)$ row by row and column by column with a symmetric low pass

filter $h = [1, 4, 6, 4, 1]/16$, resulting in a smoothed image $I_i(x, y)$. This process is repeated for J scale levels, augmenting the filter with $2^{i-1} - 1$ zeros between taps in each case. The corresponding wavelet coefficients, $W_i(x, y)$, are given as:

$$W_i(x, y) = I_{i-1}(x, y) - I_i(x, y) \quad 0 < i \leq J. \quad (6)$$

Then a hard thresholding step is applied to reduce the effect of noisy wavelet coefficients.

$$t_{hard}(W_i, t_i) = \begin{cases} W_i(x, y), & W_i(x, y) \geq t_i \\ 0, & W_i(x, y) < t_i \end{cases} \quad (7)$$

With $t_i = k\sigma_i$, where σ_i is the standard deviation of noisy wavelet coefficients at scale i and $k = 3$.

Thus, after hard thresholding, a multiscale product of each wavelet coefficient is computed to get a correlation image, $P_J(x, y)$,

$$P_J(x, y) = \prod_{i=1}^{J} W_i(x, y). \quad (8)$$

This correlation image $P_J(x, y)$, is binarized with equation (9) and the resulting connected components yield the final particles detected.

$$P_J(x, y) = \begin{cases} 255, & |P_J(x, y)| \geq l_d. \\ 0, & Otherwise \end{cases} \quad (9)$$

Where, l_d, is the predetermined detection level. A spot is accepted only at positions where the correlation is above l_d,

Feature Point Detection

The method of feature point detection was proposed in (Crocker and Grier, 1996) and used for the detection of bright particles in (Sbalzarini and Koumoutsakos, 2005). The algorithm consists of four steps:

1) **Image Restoration:** this step corrects the imperfection in the image by using a box-car average estimation and simultaneously enhances spot-like structures by convolving with a Gaussian kernel. The convolution kernel is given by:

$$K^w = \frac{1}{K_0^w} \left[\frac{1}{B} exp\left(-\frac{i^2 + j^2}{4\lambda_n^2} \right) - \frac{1}{(2w+1)^2} \right] \quad (10)$$

where K_0^w and B are normalization factors, λ_n defines the kernel width and w is a user-tunable constant, thus the final image after restoration is given by:

$$I_f(x, y) = \sum_{i=-w}^{w} \sum_{j=-w}^{w} I(x - i, y - j) K^w(i, j) \quad (11)$$

where (x, y) and (i, j) are pixel coordinates in the image and kernel, respectively.

2) **Estimating the Particle Location:** this is done by locating local intensity maxima in the filtered image, $I_f(x, y)$. A local maximum is considered to be a spot if it has the highest intensity within a local window and the intensity is in the rth highest percentile. These local maximum are identified using a gray scale dilation with a disc as the structural element. Then pixels of the filtered image with the same value as the dilation transformed image are taken as candidate locations.

3) **Refining the Particle Location:** this step reduces the standard deviation of the position measurement. It is based on the assumption that the local intensity maximum of the point P at $(\hat{x}_p, \hat{y}_p)$ is near the geometric center (x_p, y_p) of the spot. The offset is approximated by the distance to the gray-level centroid in the filtered image, $I_f(x, y)$:

$$\begin{bmatrix} \varepsilon_x(p) \\ \varepsilon_y(p) \end{bmatrix} = \frac{1}{m_0(p)} \sum_{i^2 + j^2 \leq w^2} \begin{bmatrix} i \\ j \end{bmatrix} I_f(\hat{x}_P + i, \hat{y}_p + j). \quad (12)$$

Factor $m_0(p)$, is the sum of all pixels values over feature point P given as:

$$m_0(p) = \sum_{i^2 + j^2 \leq w^2} I_f(\hat{x}_p + i, \hat{y}_p + j). \quad (13)$$

Then the refined location estimate is determined as:

$$(\tilde{x}_p, \tilde{y}_p) = (\hat{x}_p + \varepsilon_x(p), \hat{y}_p + \varepsilon_y(p)). \quad (14)$$

4) **Non-particle Discrimination:** this step rejects false identifications from sources such as auto fluorescence and dust. This step is based on the intensity moments of order 0 and 2, and identifies true particles as those within a cluster in the m_0, m_2 plane.

HDOME

The method of HDome transformation was proposed in (Vincent, 1993) and used in biological application in (Smal et al., 2010). The method is based on the mathematical morphology:

$$Hdome(I(x, y)) = I(x, y) - \rho_I(I(x, y) - h),$$

where $(I(x, y) - h)$ denotes the results of subtracting a constant, h, from a gray-scale image

$I(x, y)$, and $\rho_I(I(x, y) - h)$ is the morphological reconstruction of the gray-scale image, $I(x, y)$ from $(I(x, y) - h)$. The gray-level reconstruction is obtained by geodesic dilation of $(I(x, y) - h)$ under $I(x, y)$. The algorithm starts by reducing background noise by convolving the original gray scale image with a LoG filter and simultaneously enhancing particles. Then HDome method is applied to the filtered image to keep spots of height superior to the threshold h.